Journal of Biogeography

WILEY

Journal of Biogeography

RESEARCH ARTICLE OPEN ACCESS

Climate and Volcanic Activity Modulate Area–Distance Effects on Plant Diversity Along the Temperate–Subarctic Island Volcanic Arc

Kirill Korznikov[1] | Vyacheslav Barkalov[2] | Pavel Fibich[1,3] | Jan Altman[1,4] | Jiří Doležal[1,5]

[1]Department of Functional Ecology, Institute of Botany CAS, Třeboň, Czech Republic | [2]Federal Scientific Center for the Biodiversity of Terrestrial Biota of East Asia FEB RAS, Vladivostok, Russia | [3]Biology Centre, Institute of Entomology of the Czech Academy of Sciences, České Budějovice, Czech Republic | [4]Faculty of Forestry and Wood Sciences, Czech University of Life Sciences, Prague, Czech Republic | [5]Faculty of Science, University of South Bohemia, České Budějovice, Czech Republic

Correspondence: Kirill Korznikov (kirill.korznikov@ibot.cas.cz)

Received: 15 October 2025 | **Revised:** 25 February 2026 | **Accepted:** 27 February 2026

Keywords: biogeographical gradients | climatic filtering | habitat heterogeneity | insular floras | island biogeography | phylogenetic diversity | plant diversity drivers | volcanic activity

ABSTRACT

Aims: To evaluate how equilibrium (ETIB) and niche-based (NTIB) island-biogeography frameworks jointly explain taxonomic and phylogenetic diversity in a temperate–subarctic, volcanically active archipelago.

Location: Kuril Islands, northwestern Pacific (44°–50° N).

Time Period: Present.

Taxon: Vascular plants.

Methods: We compiled island-level floras. We quantified species richness (SR) and phylogenetic diversity metrics and related them to latitude, area, distance, a composite isolation index, elevation, volcanic bedrock cover, vegetation-type diversity and aggregated climatic indices. Analyses combined linear and second-order polynomial regressions, β-diversity partitioning, non-metric multidimensional scaling and structural equation models.

Results: Latitude emerged as the primary large-scale filter shaping both SR and phylogenetic diversity. Volcanic activity and isolation further constrained floristic diversity, together generating a pronounced mid-archipelago diversity trough. Maximal elevation was associated with higher SR but did not translate into detectable shifts in phylogenetic structure. Island area influenced diversity mainly indirectly, through its links with elevation and dispersal accessibility. Floristic differences among islands were driven predominantly by species turnover rather than nested species loss, indicating systematic replacement along the latitudinal gradient. Isolation effects were strongly non-linear, consistent with threshold-like limits to colonisation.

Main Conclusions: Area–distance relationships predicted by ETIB are strongly context-dependent. Macroclimatic filtering and long-term volcanic activity outweigh simple spatial predictors, while habitat heterogeneity exerts a secondary, modulatory role. Together, our results integrate ETIB and NTIB perspectives by showing how environmental filtering and niche availability interact in a volcanically active, temperate–subarctic island system.

1 | Introduction

The formation and diversification of flora on oceanic islands have long captivated ecologists and biogeographers. Owing to their isolation and distinctive selective regimes, islands serve as natural experiments for uncovering the mechanisms that generate and maintain biodiversity (Carlquist 1974; Whittaker et al. 2017). MacArthur and Wilson's (1967) Equilibrium Theory of Island Biogeography (ETIB) remains the conceptual basis, framing species richness (SR) as a dynamic balance between immigration and extinction governed chiefly by island area and distance from mainland source pools. Subsequent elaborations of ETIB have incorporated island geodynamics and in situ diversification (Emerson and Kolm 2005; Whittaker et al. 2008, 2017), disturbance regimes (Morrison 2010), and phylogenetic structure (Cavender-Bares et al. 2009). A growing body of work now highlights the central role of ecological niches in modulating these processes (Beaugrand et al. 2024), reviving original ideas.

Niche-focused perspectives had long lacked broad empirical support, yet recent global syntheses show that climatic and habitat-niche diversity predicts island SR across plants, herpetofauna and birds (Beaugrand et al. 2024; Blackburn et al. 2016; Jonsson et al. 2011; Stracey and Pimm 2009) and shapes the phylogenetic structure of regional floras (Qian et al. 2024). The findings underpin the emerging Niche-based Theory of Island Biogeography (NTIB), which posits that island biodiversity is a joint outcome of spatial configuration and the number, breadth and temporal turnover of ecological niches within the island matrix. The NTIB is especially pertinent to volcanic and climatically stratified archipelagos, where recurrent eruptions and rugged topography create a shifting mosaic of habitats that filter colonists and foster diversification (Stein et al. 2014).

Island size, remoteness and volcanic activity act together to shape both taxonomic and phylogenetic diversity. Larger islands typically host more species because of their broader environmental template and larger population sizes, which buffer against stochastic extinctions (Kreft et al. 2008). Conversely, small or isolated islands face low immigration rates, reduced genetic diversity and heightened sensitivity to disturbance (Gillespie et al. 2008; Kisel and Barraclough 2010). Volcanic activity compounds these trends: fresh volcanic deposits (e.g., lava, tephra or ash fields) create ecological opportunity for pioneers, yet periodic eruptions can extirpate lineages, yielding alternating signals of phylogenetic clustering and overdispersion (Nogales et al. 2022; Whittaker et al. 2017).

Latitude overlays an additional macroecological filter by shaping temperature regimes, season length and disturbance frequency (Pianka 1966; Willig et al. 2003). As conditions grow harsher toward the poles, both SR and phylogenetic dispersion generally decline, reflecting stronger environmental filtering that favours stress-tolerant, often closely related taxa (Hawkins et al. 2003; Willig et al. 2003). A continental-scale Holocene synthesis reveals that phylogenetic diversity of Asian angiosperms decreases almost linearly with latitude, underscoring the strength of climate-driven filtering across millennial time scales (Bhatta et al. 2024).

Oceanic islands provide particularly powerful natural laboratories for island biogeographic theory. Recurrent eruptions reset successional trajectories, imposing strong filters on community assembly (Whittaker et al. 2017). In situ observations from the 2021 La Palma eruption illustrate how such disturbance can simultaneously eliminate established communities while creating opportunities for recolonisation and trait-based species filtering (Nogales et al. 2022). Over evolutionary time, the interaction among volcanic disturbance, spatial isolation and steep climatic gradients has driven high levels of endemism and lineage diversification across archipelagos (Price and Clague 2002; Lim and Marshall 2017).

The Kuril Archipelago, comprising 37 active terrestrial volcanoes (68 including dormant) and extending over 1200 km between Hokkaido Island and the Kamchatka Peninsula, offers an exceptional environment for testing island-biogeographic predictions (Barkalov 2009; Gjesfjeld et al. 2019; Pietsch et al. 2003). Along this volcanic arc, the climate shifts sharply from cool-temperate in the south to subarctic climate in the north, while islands differ widely in terms of area, elevation, geological age and eruptive history (Pietsch et al. 2003). The gradients create a fine-scale mosaic of habitats, ranging from fresh volcanic deposits to mature temperate and boreal forests, that host plant assemblages at every successional stage (Barkalov 2009). Island size, isolation and volcanic disturbance intersect to shape Kuril vascular plant diversity. Larger islands provide broader environmental templates and greater demographic buffering, whereas small or remote islands experience low immigration and a heightened risk of extinction. Active volcanoes add another layer of stochasticity by periodically resetting communities while simultaneously creating new recruitment opportunities, processes expected to generate contrasting signals of phylogenetic clustering and overdispersion (Borregaard et al. 2016; Whittaker et al. 2017).

Biogeographically, the Kurils form a north–south migration corridor, but deep straits, such as the 108-km-wide Bussol Strait, have always disrupted any continuous land connections. Even during periods of lower glacial sea level, these straits remained marine, preventing the formation of terrestrial land bridges and severely limiting overland dispersal (Erlandson and Braje 2011; Pietsch et al. 2003). Palaeoecological reconstructions indicate that Holocene sea-level rise and shifting ocean currents further reinforced these barriers, promoting high island-to-island species turnover (Razjigaeva et al. 2013). Consequently, contemporary floras reflect a combination of stochastic colonisation events, environmental filtering and historical contingency (Barkalov 2009; Pietsch et al. 2003). Disentangling these drivers, therefore, demands an integrated framework that combines ecological, biogeographical and phylogenetic perspectives.

Although the high-latitude island floras have been addressed in regional syntheses (Garroutte et al. 2018; Thórhallsdóttir 2021), island biogeography remains comparatively underexplored in high-latitude regions relative to tropical and temperate systems. Particularly regarding how climatic severity and volcanic activity may shift the balance among different types of environmental filters. We examined vascular plant floras of the 20 largest islands in the Kuril Archipelago, documenting 1244 species across a pronounced temperate–subarctic climatic gradient under an oceanic monsoon regime. By integrating floristic, phylogenetic and

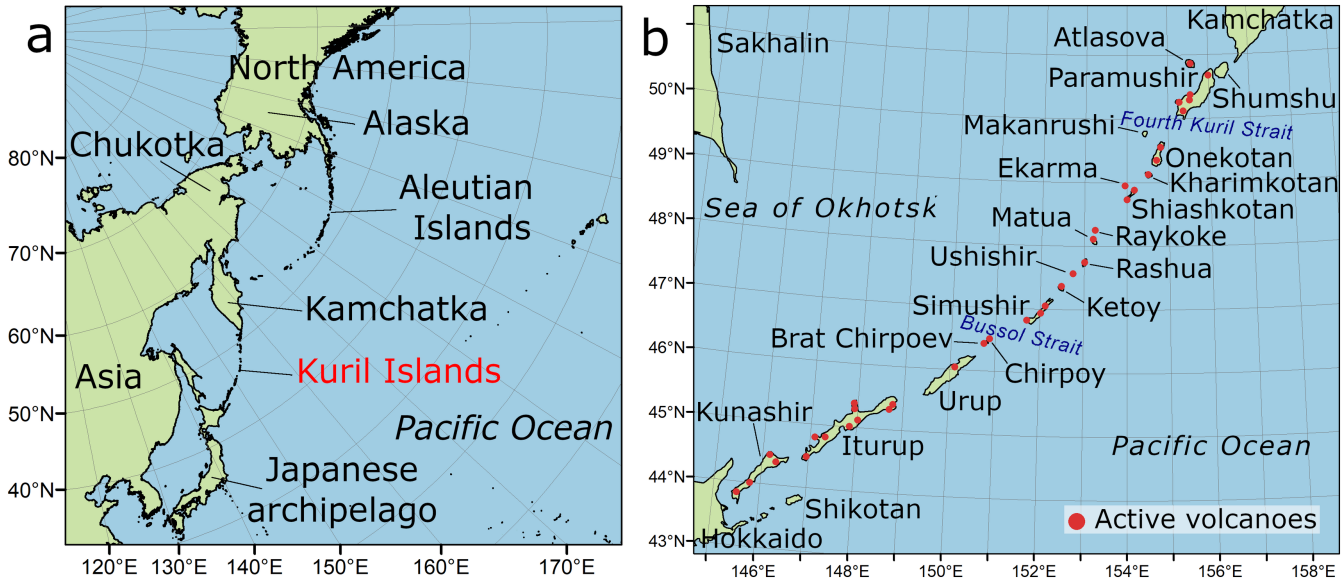

FIGURE 1 | Geographic setting of the Kuril Islands, (a) position of the Kurils within the North Pacific Island arcs, shown relative to neighbouring regions of Eurasia and North America, (b) enlarged view of the 1200-km island arc with the names of islands included in the floristic surveys.

environmental data, we evaluated how multiple environmental filters jointly structure insular plant diversity in a volcanically active island arc.

We assessed their effects using a three-tiered analytical framework: (i) multiple linear and polynomial regression models to quantify the drivers of SR; (ii) ordination of phylogenetic beta diversity to assess patterns of flora turnover along geographic and climatic gradients and (iii) structural equation modelling (SEM) to disentangle direct and indirect pathways among predictors, an approach increasingly applied in island biogeography (Blackburn et al. 2016; MacDonald et al. 2018). The combined analyses quantified the relative importance of geographic and climatic constraints and assessed the extent to which habitat heterogeneity and volcanic processes modulate classical area–isolation relationships across a latitudinal gradient (Stein et al. 2014). We tested three hypotheses: (H1) classical species–area and isolation relationships are modified along the Kuril Island arc due to increasing climatic severity toward the subarctic zone; (H2) volcanic activity acts as a long-term environmental constraint that elevates extinction risk and limits recolonisation, potentially overriding classical area–isolation effects, particularly on small and remote islands, leading to reduced SR and altered phylogenetic structure; and (H3) within the limits induced by climate and isolation, volcanism and topographical complexity increase environmental heterogeneity and thereby contribute to higher diversity by moderating large-scale geographic and climatic filters.

2 | Material and Methods

2.1 | Geographical Setting and Environmental Context

The Kuril Islands lie in the northwestern Pacific region (Figure 1a), forming part of the circum-Pacific 'Ring of Fire'. Oriented south-west to north-east over ~1200 km, the chain comprises 56 islands (Figure 1b), almost all of volcanic origin. The archipelago lies on the landward side of the Kuril–Kamchatka trench and is characterised by frequent seismic activity, including earthquake- and tsunami-generating events. Geologically, the Kurils are a classic intra-oceanic island arc developed along the leading edge of the Okhotsk microplate where the Pacific Plate subducts northwestward beneath the Kuril–Kamchatka trench (Graham et al. 2018). Arc volcanism was initiated in the Late Cretaceous, declined during the Eocene, and was rejuvenated from the Oligocene onward, producing more than 60 Quaternary stratovolcanoes that define the modern archipelago (De Grave et al. 2015). Bedrock is dominated by Neogene-Pleistocene volcanic formations (Barkalov 2009; Pietsch et al. 2003), and ongoing volcanic activities continue to reshape island topography and vegetation (Romanyuk and Degterev 2020; Romanyuk and Kordyukov 2021).

Throughout the Pleistocene, the Kuril archipelago remained insular. Even at the Last Glacial Maximum, when global sea level dropped by ~120 m, the deepest straits (e.g., between Kunashir and Iturup, Paramushir and Onekotan; Figure 1b) never emerged, preventing land bridges to either Sakhalin-Hokkaido or Kamchatka (Erlandson and Braje 2011). Although lowered sea levels temporarily enlarged individual islands and reduced inter-island distances, facilitating limited stepping-stone dispersal, continuous terrestrial connections to Eurasia were never established. Subsequent post-glacial sea-level rise (~11–8 ka) re-segmented the island chain and restored the present high-energy straits, thereby re-imposing strong marine barriers to gene flow and colonisation (Pietsch et al. 2003).

The southernmost islands lie at the boundary between the cool-temperate climate and broad-leaved forest vegetation, whereas the northernmost islands fall within the subarctic climate zone, characterised by cold summers and near-absence of forest cover (Beck et al. 2018; Barkalov 2009). The cold Oyashio Current further depresses temperatures and prolongs seasonal snow cover, rendering climatic conditions harsher

than at comparable latitudes in the eastern Pacific or Atlantic (Barkalov 2009). On southern Kunashir, the Yuzhno-Kurilsk weather station (World Meteorological Organization #32165) records a mean annual temperature of +5.1°C and 1253 mm of precipitation, of which 19% falls as snow. In contrast, the Severo-Kurilsk station on Paramushir (WMO #32215) reports a mean annual temperature of 2.8°C and 1844 mm of precipitation, with 37% occurring as snow (Figure 2b).

Steep elevational gradients superimpose local climatic variation on the broad latitudinal signal. Shumshu Island rises only to 189 m a.s.l., while neighbouring Atlasova peaks at 2339 m a.s.l. (Figure 2b), creating sharply contrasting temperature and moisture regimes among islands at similar latitudes. Natural vegetation closely reflects these climatic and topographic contrasts. Kunashir supports cool-temperate mixed forests dominated by broadleaf tree species such as *Acer mayrii* Schwer., *Quercus crispula* Blume, *Q. dentata* Thumb., and conifers *Abies sachalinensis* (F.Schmidt) Mast., *Picea jezoensis* (Siebold & Zucc.) Carrière, and an understory of dwarf bamboos (*Sasa* Makino & Shibata spp.), ferns and tall forbs. By contrast, the northern island of Paramushir is dominated by scrub communities of dwarf pine (*Pinus pumila* [Pall.] Regel), dwarf alder (*Alnus fruticosa* Rupr.) and prostrate Ericaceae shrubs, with upright trees and closed-canopy forests largely absent (Barkalov 2009).

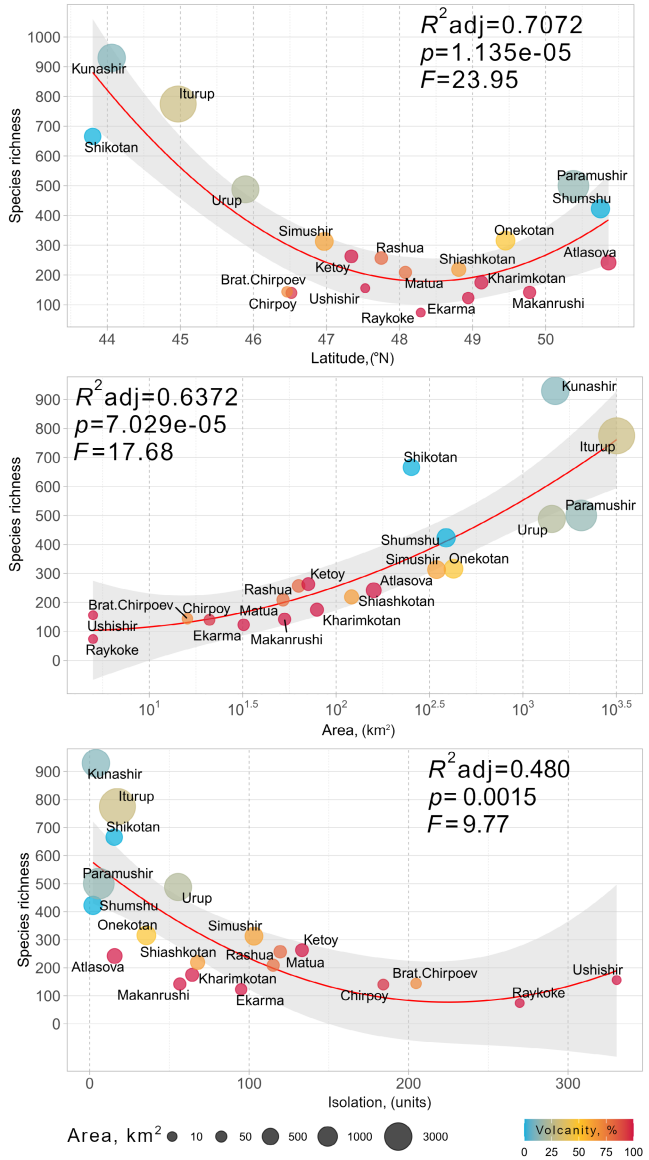

FIGURE 2 | Fitted responses of vascular plant species richness on the Kuril Islands to key environmental gradients showing significant effects (*latitude*, *area* and *isolation*). Red curves show fitted values from second-order polynomial regression models, with 95% confidence intervals (grey bands). Model comparisons indicate that quadratic terms were strongly supported for *latitude* and *isolation*, whereas support for curvature was weaker for *area* (Table S1). The fitted response to *elevation* was not statistically supported ($p = 0.3177$) and is shown in Figure S11.

2.2 | Floras and Taxonomic Concepts

The first comprehensive checklist for the middle and northern Kurils reported 879 vascular plant species (Tatewaki 1957). Subsequent syntheses raised the total to 1196 (Pietsch et al. 2003) and, most recently, to 1411 species, of which 193 are non-native in annotated flora (Barkalov 2009). Extensive field research, led by Dr. Barkalov, including participation in the International Kuril Island Project (Pietsch et al. 2003), significantly expanded the vascular plant floras of the central and northern islands (see Figures S1–S8). More than 40,000 herbarium specimens were collected during the field campaigns and deposited in several herbarium collections, including the Herbarium of Vascular Plants of the Komarov Botanical Institute (LE) and the Herbarium of the Center for the Biodiversity of Terrestrial Biota of East Asia Scientific Center of the East Asia Terrestrial Biodiversity (ex-Institute of Biology and Soil Science, VLA). In addition, we have considered the species records published after the annotated flora (Barkalov 2009) was issued (see Supporting Information S2).

For the present study, we assembled an unpublished occurrence matrix comprising 1244 native vascular plant taxa across the 30 largest Kuril Islands (7428 presence records), compiled by Dr. Barkalov. Following quality control, we excluded seven small islands south of Shikotan and three remote volcanic islands in the central archipelago because their floras were considered undersampled. These islands exhibited (i) unusually low recorded SR relative to islands of comparable size and environmental setting, and (ii) systematic absences of widespread, regionally common taxa. This pattern is most consistent with incomplete floristic coverage rather than with environmentally driven features. To minimise bias, we therefore omitted these islands from subsequent analyses. The final dataset includes 20 focal islands, spanning 10,234 km^2 and representing 97.5% of the total land area of the Kuril Archipelago.

Species circumscriptions follow Barkalov (2009) and *Vascular Plants of the Soviet (Russian) Far East* (1985–1996), both of which recognise relatively few infra-specific ranks. Consequently, some taxa treated as species may appear as sub-species or varieties in alternative taxonomic treatments. Resolving such taxonomic discrepancies is beyond the scope of our study. We aim to quantify the number of morphologically distinguishable taxa recorded in the field research. For clarity, we therefore retain the

umbrella term 'SR' throughout, even though a minority of the included morphospecies might be ranked below species level in other floras.

For each island, we quantified SR, expressed as the total number of recorded species, and phylogenetic diversity, derived from a dated phylogeny generated with the *V.PhyloMaker* package (Jin and Qian 2019) in R ver. 4.5.1 (R Core Team 2025). The phylogenetic tree was constructed using the *GBOTB.extended* megatree backbone of vascular plants, which provides branch lengths calibrated in millions of years and is based on the Angiosperm Phylogeny Group (APG IV) framework. Species absent from the backbone were assigned to their corresponding genera or families according to the default scenario '*S3*', which preserves known phylogenetic relationships and node ages.

Two complementary diversity metrics were then computed using the *picante* package (Kembel et al. 2010): mean pairwise distance (MPD) and mean nearest taxon distance (MNTD). MPD quantifies the mean phylogenetic distance among all pairs of species within an island flora and reflects overall lineage dispersion, whereas MNTD measures the mean distance between each species and its closest relative and is sensitive to phylogenetic structure near the tips of the phylogeny. To account for differences in SR among islands, both metrics were converted to standardised effect sizes (SESs, SES.MPD and SES.MNTD) using the *taxa.labels* null model (999 randomisations), which retains island-specific SR while randomising species identities across the dated phylogeny. SES values were expressed as *z*-scores calculated as the deviation of the observed metric from the null expectation divided by the null standard deviation. Positive SES values indicate phylogenetic overdispersion relative to the null model, whereas negative values indicate phylogenetic clustering. SES metrics quantify deviations from phylogenetic structure expected under a null model that preserves island-specific SR, thereby reducing the influence of richness per se on comparisons among islands.

2.3 | Environmental Drivers

To explain cross-island variation in taxonomic and phylogenetic diversity, we quantified a set of predictors commonly used in island-biogeography models. Data sources and calculation details are summarised in Table 1, and the quantitative data are provided in the Supporting Information—Supplementary_data1.csv.

Environmental drivers were selected to account for spatial constraints on colonisation, long-term environmental filtering, habitat availability and macroclimatic gradients. Latitudinal gradient was used as an integrated proxy for large-scale climatic variation across the archipelago (Pianka 1966; Willig et al. 2003; Qian and Ricklefs 2007; Beaugrand et al. 2024), reflecting strong covariation with temperature- and precipitation-based indices (Figure S9), and was therefore retained in regression analyses to avoid multicollinearity among climatic variables (see also Figure S10 for the full matrix of pairwise correlations among predictors). Macroclimate variables were used exclusively in the NMDS ordination, where they were projected as passive vectors to aid ecological interpretation without influencing the ordination structure.

Island area, distance to the mainland, and the composite isolation index were used to represent the classical species–area and dispersal limitation effects (MacArthur and Wilson 1967; Lomolino 2000; MacDonald et al. 2018). Maximum elevation was included as a proxy for vertical environmental gradients (Körner 2007; Steinbauer et al. 2016) and for potential niche diversification within islands (Stein et al. 2014). Vegetation heterogeneity was quantified using a Shannon diversity index derived from mapped vegetation units and was used as a coarse proxy for habitat heterogeneity by summarising the diversity of environmental settings across an island, which may facilitate species coexistence through niche differentiation.

Volcanic bedrock cover was included as a proxy for island geodynamics, reflecting the long-term geological nature of island systems as emphasised in general dynamic models of island biogeography (Whittaker et al. 2008, 2017). This environmental driver quantifies the proportion of island surface composed of Pleistocene–Holocene volcanic substrates and therefore captures persistent geological activity, substrate renewal and soil development constraints operating over both evolutionary and ecological timescales, rather than only short-lived eruptive events (Nogales et al. 2022; Romanyuk and Degterev 2020). High volcanic bedrock cover is expected to influence plant communities by limiting soil depth and stability, periodically resetting successional trajectories, and constraining habitat continuity (Romanyuk and Kordyukov 2021), thereby acting as a long-term geological filter on SR and phylogenetic structure.

Our analyses focused on natural environmental gradients shaping native vascular-plant floras. Accordingly, the models target persistent, spatially structured drivers that can be quantified consistently across all islands. Anthropogenic influence was not included as a predictor because most analysed islands are uninhabited or only minimally modified, and because no consistent, floristically meaningful index of human disturbance is available at the archipelago scale. Although human activities can strongly affect island biotas in densely populated systems (Garroutte et al. 2018; Helmus et al. 2014), they are unlikely to constitute a primary floristic filter in the largely uninhabited Kuril Islands.

2.4 | Statistical Analyses

2.4.1 | Visualisation of Fitted Responses

We used bivariate scatterplots to visualise observed variation in SR, SES.MNTD and SES.MPD along individual environmental gradients. We produced all visualisations in R ver. 4.5.1 (R Core Team 2025) using the *ggplot2* package (Wickham 2016), with fitted curves generated using the second-order polynomial linear models specified as $y \sim \text{poly}(x, 2)$. To formally assess whether curvature was supported, we compared each second-order polynomial model against its linear counterpart ($y \sim x$) using small-sample corrected Akaike Information Criterion (AIC) and nested-model *F*-tests for the additional quadratic term (results are summarised in Table S1). The bivariate scatterplots were intended to illustrate responses along individual gradients and

TABLE 1 | Predictors used in analyses.

Context	Variable	Code	Description
Spatial	Area (km^2)	*Area*	Polygon areas rounded to the nearest km^2
	Mainland distance (km)	*Distance*	Shortest great-circle distance from the island shoreline to Hokkaido or the Kamchatka Peninsula, measured in Google Earth Pro programme
	Composite isolation index	*Isolation*	$\text{Isolation} = \frac{\log_{10}(\text{distance}_{km})}{\sqrt{\text{Area}_{km^2}}}$; low values denote weak isolation
	Latitude (° N)	*Latitude*	Geographical position of the island's geometrical centre, rounded to two decimal places
Topography and habitat heterogeneity	Maximum elevation (m a.s.l.)	*Elevation*	Highest altitude derived from the topographic maps
Geodynamism	Volcanic bedrock cover (%)	*Volcanity*	Proportion of island surface mapped as Pleistocene–Holocene volcanic bedrocks in the geological map of the Kuril Islands 1:2,000,000 (*Atlas of the Kuril Islands* 2009) indicates long-term exposure to volcanic substrates rather than very recent lava/tephra deposits
Habitat heterogeneity	Vegetation Shannon index (H')	*Vegetation*	Proportion of 26 vegetation units derived from the Vegetation map of the Kuril Islands 1:2,000,000 (*Atlas of the Kuril Islands* 2009) and computed Shannon's index (natural logarithm) $H' = -\sum_{i=1}^{26} p_i \times \ln\ p_i$ with the convention $0\ln 0 = 0$.
Macroclimate[a] (Nakamura et al. 2007)	Kira's warmth Index	*KWI*	$\text{KWI} = \sum_{i=1}^{12} \max\left(0, T_i - 5\right) \times 10$
	Kira's coldness Index	*KCI*	$\text{KWI} = \sum_{i=1}^{12} \min\left(0, T_i\right) \times 10$
	Seasonal rain precipitation (mm)	*Rain*	$P_{\text{pos}} = \sum P_i \text{ where } T_i > 0°\text{C}$
	Seasonal snow precipitation (mm)	*Snow*	$P_{\text{neg}} = \sum P_i \text{ where } T_i < 0°\text{C}$

[a]Monthly temperature T_i and precipitation P_i were derived from WorldClim 2.1 (Fick and Hijmans 2017) datasets at 30-arc-second resolution and averaged spatially within the boundaries of each island.

should not be interpreted as exploratory smoothers or independent tests of non-linearity.

2.4.2 | Nestedness and Turnover

We partitioned β-diversity into turnover (species replacement among floras) and nestedness (richness differences where species-poor floras are proper subsets of richer ones) using functions *nestedbetajac* (Jaccard) and *nestedbetasor* (Sørensen) in R ver. 4.5.1 (R Core Team 2025) the package *vegan* (Baselga 2010; Oksanen et al. 2022; Steinbauer et al. 2016). Using both indices ensures patterns are not artefacts of a single weighting scheme. Analyses used a 20×1244 (islands×species) binary presence–absence matrix (Supporting Information—Supplementary_data2.csv). Significance of turnover and nestedness was evaluated with 999 null communities via the function *oecosimu* under the fixed-row, equiprobable-column algorithm (island richness fixed, each species equally likely on any island). We also assessed checkerboard structure with the function *nestedchecker* under the same null model. The data matrix and R codes are available in the Supporting Information—Supplementary_code1.txt.

2.4.3 | NMDS Ordination

We analysed the same islands×species presence–absence matrix using non-metric multi-dimensional scaling (NMDS; Bray–Curtis dissimilarity, two dimensions) implemented in the *metaMDS* function, the package *vegan* (Oksanen et al. 2022) in R ver. 4.5.1 (R Core Team 2025). To visualise phytogeographical composition of island floras, we assigned every species to one of six distribution types (Asio-American, Asian, Insular, Amphipacific, Circumpolar and Eurasian) updated from Barkalov (2009), using species occurrence maps available on Plants of the World Online (POWO 2025) (Table S2). To relate floristic composition to the environment, we fitted island-level predictors using *envfit* with 999 permutations. Smooth isolines for SR and the phytogeographical distribution types were added with the function *ordisurf* (thin-plate spline). The R code is available in the Supporting Information—Supplementary_code2.txt.

2.4.4 | Regression and Penalised Models

We quantified associations between environmental predictors and SR, SES.MNTD and SES.MPD, using multiple regression models. To accommodate evident non-linear relationships, we allowed second-order polynomial terms for selected predictors and retained them only when supported by information-theoretical criteria. Model selection was conducted using an information-theoretic approach based on AIC, implemented via stepwise backward selection using the function *stepAIC* in the package *MASS* (Venables and Ripley 2002) in R ver. 4.5.1 (R Core Team 2025), starting from a predefined full model. This procedure was used to identify a parsimonious model that summarises the dominant associations present in the data, rather than to discover predictors de novo. The stepAIC-selected first-order (linear) model is reported as a basic model for interpretation. Then, to evaluate potential non-linearities and the robustness of variable importance and functional form, we additionally considered second-order (polynomial) specifications. We first performed stepwise AIC selection from a global polynomial model and assessed collinearity by calculating the generalised variance inflation factor (GVIF). Where the GVIF indicated substantial collinearity, we restricted the candidate predictor set accordingly before applying cross-validated lasso regression using the function *cv.glmnet* in the package *glmnet* (Friedman et al. 2010, 2025). Thus, coefficients for the resulting polynomial model were obtained by refitting an ordinary least squares (OLSs) model with the lasso-retained terms.

We evaluated model adequacy using the following diagnostic procedures. We inspected residual patterns and influential observations for all models. We additionally assessed residual normality (Q–Q plots) and homoscedasticity (residuals vs. fitted values). Collinearity among predictors was quantified using GVIF via the function *vif* in the package *car* (Fox and Weisberg 2019), interpreted as $GVIF^{1/2\times df}$, with values of 2–3 indicating moderate and >3 high collinearity (Fox and Weisberg 2019). For OLS models, coefficient *p*-values were computed using two-sided Wald *t*-tests, with degrees of freedom equal to the residual df reported for each model. The R code is available in the Supporting Information—Supplementary_code3.txt.

2.4.5 | Structural Equation Models

We used SEM (Grace et al. 2010) to evaluate hypothesized direct and indirect pathways linking island geography, macroclimate, volcanic activity and topographic structure to patterns of vascular plant diversity across the archipelago. SEM is particularly suitable in this context because key predictors are intercorrelated (Figure S10) and may influence SR both directly and indirectly through mediation (e.g., climate shaping environmental templates, or geodynamic influence on topographic structure and habitat continuity). Accordingly, SEM was used to assess whether the observed covariance structure is consistent with a hypothesized process-based organisation, rather than to infer isolated causal effects.

The conceptual model assumed that (i) *area* and *isolation* constrain immigration and extinction rates and thus can affect SR directly; (ii) macroclimate limits the regional species pool and establishment success and can also influence habitat configuration; (iii) topographic structure (*elevation*) contributes to environmental gradients and potential habitat diversity; (iv) vegetation heterogeneity (*vegetation*) reflects the availability of major habitat types and may mediate effects of area, climate, and topography and (v) *volcanity* represents geodynamic processes and long-term substrate renewal, expected to influence diversity both directly (through edaphic and disturbance constraints) and indirectly through its effects on habitat templates. We specified directional links only where ecological directionality is unambiguous (e.g., island area does not depend on SR), while reciprocal or biologically implausible pathways were avoided. Because many predictors represent interacting components of the same island system, paths are interpreted as dominant process directions rather than isolated causal effects.

Given the strong correlations among predictors and the limited sample size ($n=20$ islands), we implemented the core SEM focusing on a parsimonious subset of dominant predictors: *area*, *latitude*, *distance*, *elevation* and *volcanity*. This reduced model was designed to minimise multicollinearity (VIF <3) and to provide stable parameter estimates while retaining the core processes represented in the conceptual framework. A limited number of ecologically motivated interaction terms were included to capture hypothesized joint effects among key drivers.

We implemented piecewise SEM using the *psem* function in the package *piecewiseSEM* (Lefcheck 2016) in R ver. 4.5.1 (R Core Team 2025). Each component relationship was fitted using OLS regression after appropriate transformations (log or *z*-scaling) to improve normality and place coefficients on comparable scales. Separate SEMs were fitted for each focal response variable (SR, SES.MNTD and SES.MPD), using the same structural framework while substituting the response variable in the terminal equation.

Model fit was evaluated using tests of directed separation summarised by Fisher's *C*, which assesses whether the conditional independence claims implied by the conceptual model are consistent with the observed data. We reported standardised path coefficients (β) and R^2 values for each endogenous variable. Results from the core SEM are presented in the main text, whereas the full SEM, including all theoretically motivated predictors, is provided in the Supporting Information to illustrate the complete conceptual structure. The R code for both SEMs is available in the Supporting Information—Supplementary_code4.txt and Supplementary_code5.txt.

3 | Results

3.1 | Bivariate Scatterplots

The selected models include second-order polynomial terms, resulting in pronounced curvilinear fitted responses. However, formal comparisons of linear ($y\sim x$) versus second-order polynomial models showed that support for curvature differed among response variables and predictors (Table S1). SR showed clear, statistically robust responses to the *latitude*, *area* and *isolation* (Figure 2). The mid-archipelago trough corresponded to the cluster of small, highly volcanic islands (e.g., Kharimkotan, Ketoy, Rashua; Figures S5–S7) whose limited *area*, high *isolation* and

high *volcanity* jointly depressed SR. Rich assemblages re-emerged on the large northern islands close to Kamchatka (Paramushir, Shumshu; Figure S8), indicating that the *latitude* effect was modulated by island attributes rather than driven by *latitude* alone.

SR increased with *area*, with evidence for curvature that was weak to moderate in model comparisons (Table S1). Islands smaller than 50 km^2 rarely exceed 250 species, whereas islands larger than 1000 km^2 approach or surpass 900 species. SR decreased with the *isolation*: near-mainland islands (less than 50 units) host 300–950 species, whereas the most remote central volcanoes (less than 200–300 units) rarely exceed 150–200 species. Although the polynomial smoother showed a slight upturn beyond ~250 units, confidence bands were wide, and the trend was overwhelmingly negative across the observed range. *Elevation* explained little residual variance; for example, Atlasova Island (Figure S8) remains species-poor, underscoring that steep topography and high elevation did not compensate for all other drivers (Figure S11).

Both phylogenetic metrics show parallel, but statistically tighter, latitudinal gradients (Figure 3). SES.MNTD decreases almost linearly with *latitude*, signalling stronger environmental filtering toward the sub-arctic end of the island chain. SES.MPD reveals the same pattern, implying that entire lineages, not just close relatives, are selectively excluded in colder climates. Consistent with this visual impression, linear–polynomial comparisons generally favoured linear models for SES.MNTD, whereas SES.MPD showed mixed support for quadratic terms depending on the predictor (Table S1). By contrast, *area* and *elevation* exert weak or non-significant effects on phylogenetic structure (Figure S12). *Isolation* shows a significant influence on SES.MPD but not on SES.MNTD (Figure S12), consistent with immigration limitation reducing deep-lineage representation on the remotest islands.

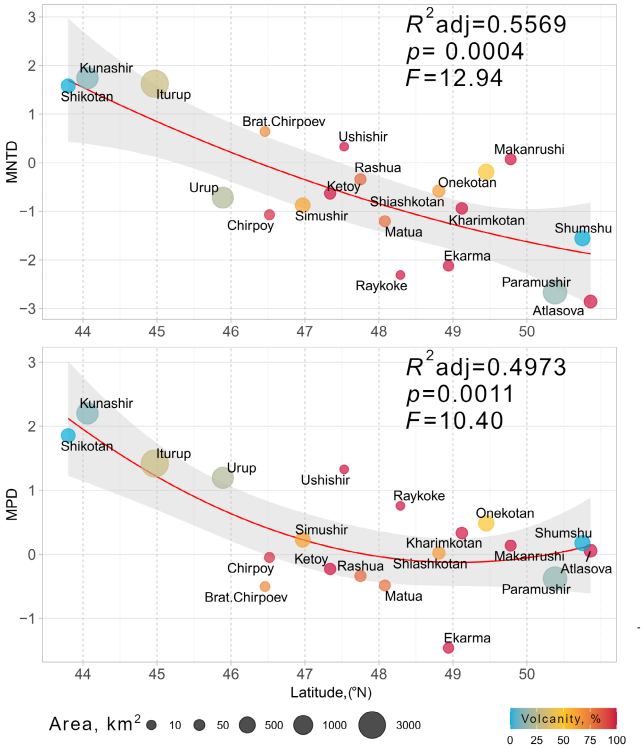

FIGURE 3 | Fitted responses of phylogenetic diversity of vascular plant floras on the Kuril Islands, expressed as standardised mean nearest taxon distance (SES.MNTD) and mean pairwise distance (SES.MPD) to the latitudinal gradient. Red curves represent second-degree polynomial fits with 95% confidence intervals (grey bands). Linear models were preferred, notably for SES.MNTD, the quadratic fit provides an effective linear visualisation (formal comparisons are reported in Table S1). Responses to *area*, *isolation* and *elevation* ($p < 0.05$) are shown in Figure S12.

3.2 | Compositional Gradients and Phytogeography

The NMDS ordination (Figure 4) revealed a pronounced gradient in floristic composition across the Kuril Islands, with this compositional turnover closely aligned with variation in SR. Southern islands (Iturup, Kunashir, Shikotan; Figures S1–S3) occupied the positive region of NMDS1 and NMDS2 and are associated with higher *KWI* values, greater *area* and *rain*. In contrast, the small, cold and highly volcanic islands of the central archipelago cluster are placed on the ordination centre, indicating broadly similar species-poor floras. The northernmost islands (Atlasova, Paramushir, Shumshu; Figure S8) are displaced toward the negative extreme of NMDS2, where vectors for *latitude*, *snow* and *KCI* indicate stronger climatic filtering.

The NMDS was partitioned by the phytogeographical distribution types of vascular plant species (Figure 4b). Asian taxa dominated the warm, southern sector and diminished sharply northward. Asio-American species peaked in the central-archipelago cluster, then remained abundant on the northern islands. Circumpolar species increased monotonically toward the subarctic end of the gradient, consistent with broader high-latitude floras. Insular endemics varied little across the Kurils but attained their highest percentages on the southern islands.

Partitioning of β-diversity showed that community change across the archipelago was dominated by species turnover rather than ordered species loss. Using Jaccard dissimilarity, we found $\beta_{turnover} = 0.73$ and $\beta_{nestedness} = 0.19$, and Sørensen dissimilarity showed $\beta_{turnover} = 0.58$ and $\beta_{nestedness} = 0.28$ (all $p < 0.01$ vs. null communities). Thus, most compositional variation reflected replacement along environmental gradients. The Kuril floras also exhibited significantly fewer checkerboard pairs than expected under the fixed-row, equiprobable-column null model (*C*-score SES = −27.0, $p = 0.001$), indicating greater co-occurrence (aggregation) than chance (Figure 5), consistent with environmentally filtered, partially nested assembly rather than widespread competitive exclusion. Collectively, the results indicated that floras of northern and central islands are not merely impoverished subsets of southern floras but represent distinct species pools.

3.3 | Linear Models

Model selection using AIC identified a consistent set of predictors for SR, including *latitude*, *volcanity*, *distance*, *elevation*

and *area* (Table 2; Figures S13a–S15a), together explaining 93% of the across-island variance. Linear models for both SES.MNTD and SES.MPD retained fewer predictors, but *latitude* remained the dominant explanatory variable, indicating a consistent latitudinal signal across taxonomic and phylogenetic dimensions.

In this linear framework, *latitude* exhibited the strongest statistical support (largest absolute *t* value) and the largest unique contribution to SR (derived partial $R^2 = 0.74$), followed by *distance* (partial $R^2 = 0.52$) and *volcanity* (partial $R^2 = 0.47$). *Distance* and *volcanity* showed significant negative effects, while *elevation* had a modest positive association (partial $R^2 = 0.28$). *Area* was positive but not statistically supported once the other covariates were included (partial $R^2 = 016$).

3.4 | Polynomial Models

For SR, the second-order polynomial model selected using penalised lasso regression retained *latitude*, *elevation*, *volcanity* and *isolation* (Table 3; Figures S13b–S15b). The significant quadratic term for *isolation* indicated a concave response, with SR declining sharply with increasing *isolation* up to an intermediate threshold, beyond which further *isolation* produces diminishing additional losses. This pattern was not detectable in the linear framework and highlights a threshold-like constraint. The lasso selection retained only the linear term of *latitude* for SES.MNTD. The linear term of *latitude* with linear and quadratic terms of *isolation* was retained for SES.MPD. Models explained 79% (SES.MPD) and 63% (SES.MNTD) of the variance (Table 3). Polynomial models complement linear analyses by revealing response shape and

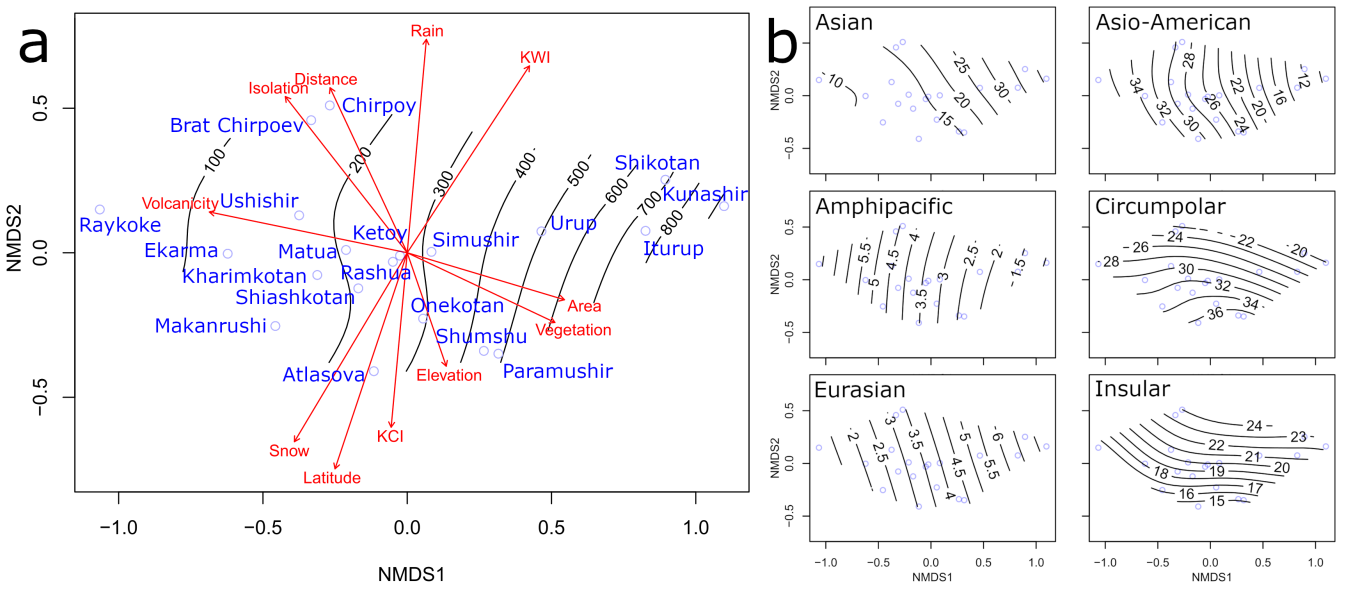

FIGURE 4 | The floristic composition and environmental predictors across the Kuril Islands illustrate the latitude-driven climate, isolation and volcanic activity structure both overall diversity and the phytogeographical provenance of the Kuril Island floras; (a) two-dimensional NMDS ordination (stress = 0.05) of the 20 island floras (blue circles, labelled), red vectors show fitted environmental predictors, black isolines indicate thin-plate-spline contours of species richness (numbers equal predicted species); (b) contour maps of the same NMDS space depicting the percentage contribution of six phytogeographical distribution types, higher contour values denote greater representation of the focal type in island floras occupying that sector of ordination space.

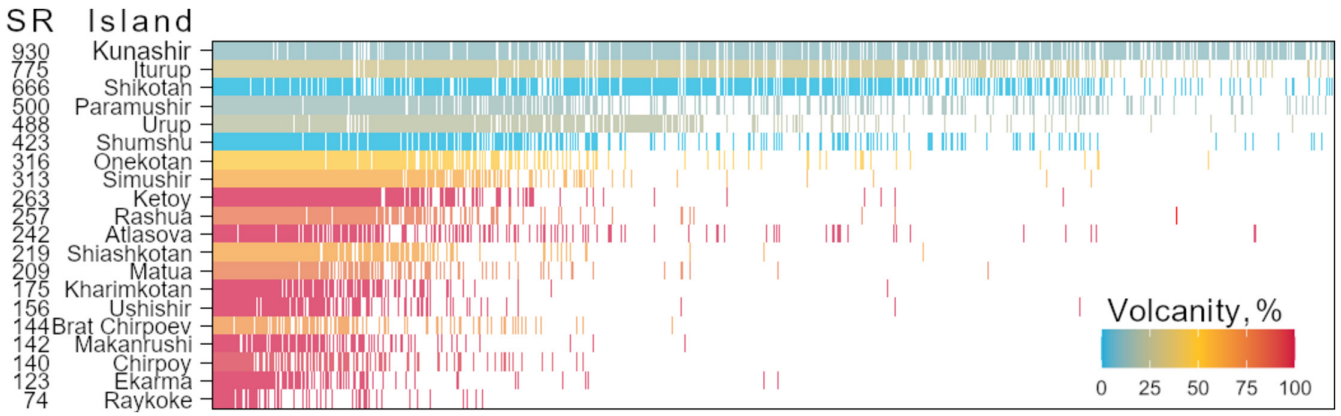

FIGURE 5 | Island-by-species composition matrix ordered by descending richness, vertical ticks represent individual species. SR, species richness.

TABLE 2 | AIC-supported multiple-linear models for species richness (SR), standardised mean nearest taxon distance (SES.MNTD) and standardised mean pairwise distance (SES.MPD).

Predictor	Estimate	SE	*t*-value	*p*
SR[a]				
Intercept	3031.29	407.34	7.44	3.2×10^{-6}***
Area	0.042	0.0258	1.64	0.124
Latitude	−53.13	8.43	−6.30	1.9×10^{-5}***
Elevation	0.0738	0.0319	2.32	0.036*
Volcanity	−2.216	0.628	−3.53	0.0033**
Distance	−0.464	0.119	−3.89	0.0017**
SES.MNTD[b]				
Intercept	31.34	5.66	5.54	4.5×10^{-5}***
Latitude	−0.615	0.105	−5.88	2.3×10^{-5}***
Isolation	−0.0073	0.0033	−2.19	0.043*
Vegetation	−1.376	0.654	−2.10	0.052****
SES.MPD[c]				
Intercept	15.71	3.11	5.05	1.2×10^{-4}***
Latitude	−0.307	0.064	−4.79	2.0×10^{-4}***
Isolation	0.0044	0.0023	1.94	0.070****
Distance	−0.0040	0.0012	−3.42	0.0035**

Note: Reported coefficients are unstandardized ordinary least squares (OLS) estimates, with associated standard errors, *t*-values and two-sided Wald *p*-values.
[a]Residual SE = 60.08 (df = 14), multiple $R^2 = 0.952$, adjusted $R^2 = 0.935$, overall $F(5, 14) = 55.2$, $p = 1.0\times10^{-8}$.
[b]Residual SE = 0.818 (df = 16), multiple $R^2 = 0.690$, adjusted $R^2 = 0.632$, overall $F(3, 16) = 11.9$, $p = 2.4\times10^{-4}$.
[c]Residual SE = 0.57 (df = 16), multiple $R^2 = 0.658$, adjusted $R^2 = 0.593$, overall $F(3, 16) = 10.24$, $p = 5.3\times10^{-4}$.
*< 0.05: *p*-value significance.
**< 0.01: *p*-value significance.
***< 0.001: *p*-value significance.
****< 0.10: *p*-value significance.

TABLE 3 | Final second-order polynomial regression models for species richness (SR), standardised mean nearest taxon distance (SES.MNTD) and standardised mean pairwise distance (SES.MPD).

Predictor	Estimate	SE	*t*-value	*p*
SR[a]				
Intercept	327.75	13.11	25.00	5.1×10^{-13}***
Latitude[1]	−521.35	73.40	−7.10	5.3×10^{-6}***
Elevation[1]	194.48	77.25	2.51	0.0246*
Volcanity[1]	−322.80	115.38	−2.79	0.0142*
Isolation[1]	−377.09	114.95	−3.28	0.00547**
Isolation[2]	304.72	71.60	4.25	7.99×10^{-4}***
SES.MNTD[b]				
Intercept	−0.603	0.199	−3.04	0.007
Latitude[1]	−4.519	0.888	−5.09	7.65×10^{-5}***
SES.MPD[c]				
Intercept	−0.603	0.200	−3.01	0.008**
Latitude[1]	−4.590	0.898	−5.11	1.0×10^{-4}***
Isolation[1]	−0.717	0.898	−0.80	0.436
Isolation[2]	0.935	0.895	1.05	0.312

Note: Candidate predictors were first screened using stepwise AIC on a global polynomial model; due to elevated collinearity (GVIF), a reduced predictor subset was then evaluated using cross-validated lasso to select retained linear[1] and quadratic[2] terms. Reported coefficients are unstandardized ordinary least squares (OLS) estimates from the refitted model, with corresponding *t*-values and two-sided Wald *p*-values.
[a]Residual SE = 58.62 (df = 14); multiple $R^2 = 0.954$; adjusted $R^2 = 0.938$; overall $F(5, 14) = 58.15$, $p = 7.23\times10^{-9}$.
[b]Residual SE = 0.888 (df = 18); multiple $R^2 = 0.590$; adjusted $R^2 = 0.567$; overall $F(1, 18) = 25.9$, $p = 7.65\times10^{-5}$.
[c]Residual SE = 0.445 (df = 16); multiple $R^2 = 0.791$; adjusted $R^2 = 0.752$; overall $F(3, 16) = 20.2$, $p = 1.1\times10^{-5}$.
*< 0.05: *p*-value significance.
**< 0.01: *p*-value significance.
***< 0.001: *p*-value significance.

potential thresholds, while reinforcing the dominant role of latitudinal filtering for SR, SES.MNTD and SES.MPD.

3.5 | Structural Equation Models

The same five predictors retained in the linear models were used as variables in the core SEMs. Fisher's *C* indicated good global fit for all models ($C = 3.02$, $p = 0.806$); variance explained is high for SR ($R^2 = 0.95$) and moderate for SES.MNTD ($R^2 = 0.65$) and SES.MPD ($R^2 = 0.59$) (Figure 6; Table S3).

SR showed strong negative direct effects of *latitude* ($\beta = -0.47$, $p < 0.001$) and *volcanity* ($\beta = -0.36$, $p = 0.003$), consistent with climate and substrate filtering. *Distance* also had a negative effect ($\beta = -0.35$, $p = 0.002$), indicating immigration limitation. *Elevation* exerted a small positive effect ($\beta = 0.17$, $p = 0.036$), whereas the direct path from *area* was not significant ($\beta = 0.15$, $p = 0.124$), implying that island size influences SR primarily indirectly rather than through a simple species–area mechanism.

For phylogenetic structure, both SES.MNTD and SES.MPD declined with *latitude* ($\beta = -0.83$, $p = 0.001$ and $\beta = -0.69$, $p = 0.006$), indicating stronger environmental filtering toward the north that reduces both close-tip clustering (SES.MNTD) and deep lineage breadth (SES.MPD). In contrast, direct effects of *volcanity* on SES.MNTD and SES.MPD were not significant (β ~0.10–0.12, $p \geq 0.66$). The direct effect of *elevation* on SES.MNTD also was not significant ($\beta = -0.19$, $p = 0.37$), and neither phylogenetic metric retained significant direct dependence on *area* or *distance* once *latitude* (and, for SR, *volcanity* and *distance*) is accounted for. Notably, *volcanity* strongly corresponded with *area* ($\beta = -0.60$, $p = 0.001$) and *elevation* corresponded with *area* ($\beta = 0.45$, $p = 0.012$), underscoring indirect pathways among predictors.

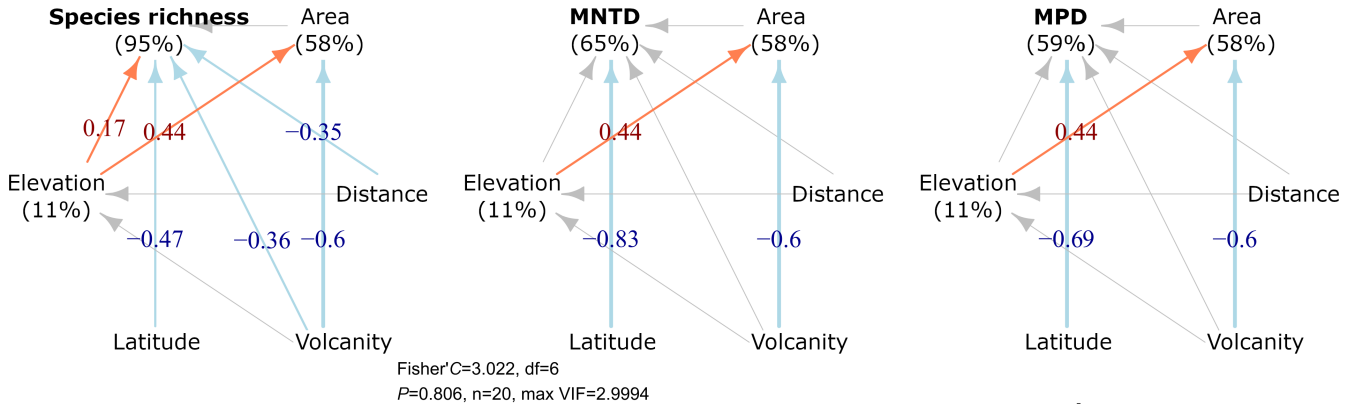

FIGURE 6 | Structural-equation models (SEMs) linking predictor variables to species richness (SR) standardised mean nearest taxon distance (SES.MNTD), and standardised mean pairwise distance (SES.MPD) on the Kuril Islands; arrows represent relationships, red—positive effect, blue—negative effect, grey—non-significant; numbers on arrows are standardised path coefficients (β); percentage values give the proportion of variance explained (marginal R^2).

The full SEMs, including the full set of predictors, yielded global fits indicating that some conditional independences were violated (all Fisher's $C > 129$, $p < 0.001$), reflecting residual associations among predictors (Figure S16; Table S4). Nevertheless, the individual path coefficients were well supported and consistent with the hypothesized causal structure. *Latitude* was not modelled as a direct predictor of SR, SES.MNTD and SES.MPD, but exerted strong indirect effects through its influence on the climatic variables *KWI* and *snow*. In the model, SR ($R^2 = 0.94$) increased with *KWI* ($\beta = 0.72$, $p = 0.015$) and declined with *volcanity* ($\beta = -0.38$, $p = 0.019$), whereas other direct effects were weak or non-significant. SES.MNTD ($R^2 = 0.69$) was significantly and positively associated with *KWI* ($\beta = 1.86$, $p = 0.008$), while SES.MPD ($R^2 = 0.61$) showed no significant direct predictors.

4 | Discussion

4.1 | Discussion of Hypotheses

The Kuril Islands represent a textbook 'natural experiment' (Whittaker et al. 2017) in which geographic position, island size, isolation and volcanic activity co-vary across nearly 6° of latitude, spanning temperate to subarctic climatic conditions. By explicitly modelling those covariates, we identify three broad patterns. First, both taxonomic and phylogenetic diversity decline poleward, reflecting strong latitudinal climatic filtering. Second, small, remote and highly volcanic islands are disproportionately depauperated, consistent with combined dispersal limitation and long-term geodynamic constraints on carrying capacity. Third, topographic complexity (expressed through elevational gradient and associated vertical habitat zonation) contributes positively to SR, although its effect is weaker than, and partially contingent on, large-scale climatic and geographic constraints. Rather than acting independently of latitude or size, vertical environmental heterogeneity appears to modulate local diversity by expanding niche availability within the limits imposed by climate and isolation. Below, we discuss each pattern in turn, placing the Kuril Islands flora in a broader biogeographic context.

4.1.1 | H1 Latitudinal Declines in Species and Phylogenetic Diversity

In accordance with H1, both SR and phylogenetic diversity declined along the south–north latitudinal gradient, although with contrasting response shapes. SR exhibits a pronounced mid-archipelago trough, where the smallest, most volcanic islands are located, whereas phylogenetic diversity declines almost linearly (Figures 2 and 3). This tight latitudinal signal aligns with global angiosperm data sets, in which phylogenetic dispersion declines steadily toward the poles, resulting in assemblages that are increasingly composed of closely related, stress-tolerant lineages (Bhatta et al. 2024).

NMDS ordination reinforces the latitudinal gradient: warm, high-rainfall islands (Kunashir, Iturup) cluster at one extreme, while cold, snow-dominated islands (Paramushir, Shumshu) occupy the other (Figure 4a). The accompanying turnover-nestedness decomposition shows that β-diversity is driven overwhelmingly by species turnover rather than nested species loss, that is, more northern floras are not impoverished subsets of southern floras. Phytogeographically, this shift is expressed as a transition from floras rich in East-Asian species on the southern islands to Asio–American (Beringian) species in the central part and an increasing circumpolar component in the north (Figure 4b). The pattern accords with well-known dispersal filters imposed by the deep Bussol and Fourth Kuril straits (Figure 2b), augmented by a northward increase in climatic severity.

The Kuril Islands also differ from many oceanic archipelagos in their proximity to continental floras, with southern islands showing stronger affinities to Japan (Hokkaido Island) and northern islands to the Kamchatka Peninsula, adding a historical and biogeographic dimension to latitudinal filtering and re-colonisation dynamics. A close analogue is the Aleutian–Commander Island chain (Garroutte et al. 2018), which is similarly placed between Alaska and Kamchatka (Figure 1a), but is structured primarily along an east–west direction. In the Kurils, latitude therefore acts as a composite proxy predictor that integrates temperature regime, rain precipitation and snow

accumulation (Figure S9), capturing the strong environmental filters in Northeast Asia (Nakamura et al. 2007).

Phylogenetic diversity metrics add an essential evolutionary dimension to the SR gradient. Whereas SR showed a pronounced mid-archipelago trough, SES.MNTD declined almost linearly with *latitude*, while SES.MPD also decreased poleward but with a weaker non-linear component than SR (Figure 3). This pattern accords with the energy-diversity hypothesis (Allen et al. 2002; Qian and Ricklefs 2007): warm, productive southern islands sustain more evolutionary breadth and ecological specialisation, whereas colder, less productive northern islands favour a limited set of cold-adapted clades.

4.1.2 | H2 Isolation, Volcanic Activity and the Central-Island Bottleneck

Our second hypothesis is supported by both regression and SEM results, which together indicate that volcanic activity constrains island floras through multiple pathways. In the SEMs, *volcanity* shows a direct negative effect on SR, consistent with long-term geodynamical disturbance limiting soil development, constraining succession and elevating local extinction risk. In the core SEM, *volcanity* is also strongly associated with island area, indicating that more volcanic islands in the Kurils tended to be smaller, but this pathway is not translated into a statistically supported indirect effect on SR.

For phylogenetic structure, *volcanity* does not show a detectable direct effect. Instead, phylogenetic patterns are dominated by the latitudinal climatic gradient and, to a lesser extent, geographic remoteness. This suggests that volcanic activity in the Kurils primarily reduces local richness, while phylogenetic structure is shaped more strongly by broad climatic filtering and dispersal constraints. Over longer timescales, repeated disturbance may still contribute to lineage filtering by favouring clades able to persist and recolonize disturbed islands, but our SEM results did not isolate a strong *volcanity*-driven pathway for phylogenetic structure. Although SES.MNTD and SES.MPD show broadly similar latitudinal patterns to each other, their response structure differs from SR: richness shows a pronounced mid-archipelago trough and stronger responses to *volcanism* and *isolation*, whereas phylogenetic metrics are dominated by the latitudinal climatic gradient and show weaker direct *volcanity* effects.

This pattern is consistent with many studies showing that frequent disturbance can suppress species accumulation and, over longer timescales, act as a selective filter on lineages with limited dispersal or narrow ecological tolerances (Borregaard et al. 2016; Whittaker et al. 2008; Nogales et al. 2022). At the same time, volcanic systems are not purely destructive. Our results are compatible with the idea that volcanic landscapes can introduce spatial and temporal heterogeneity at the archipelago scale, potentially promoting β-diversity and lineage turnover even as α-diversity on individual islands remains low (Price and Clague 2002). Geothermal environments may further act as micro-refugia that buffer temperature extremes and allow thermophilic or relict taxa to persist beyond their regional climatic envelopes (Stein et al. 2014), as illustrated by the occurrence of *Psilotum nudum* (L.) P.Beauv. on Kunashir (Barkalov and Yakubov 2007). The balance between these destructive and constructive roles is therefore likely to differ across taxonomic and phylogenetic dimensions and to shift between ecological (decadal) and evolutionary (millennial) timescales.

Isolation further amplified this central-archipelago bottleneck. Because the isolation index integrates both distance to the mainland and island size, it captures dispersal limitation differently from raw distance to the mainland alone. In the linear model, distance to the nearest mainland emerged as a significant negative predictor of SR, reflecting reduced colonisation with increasing remoteness. When remoteness was expressed as a composite isolation index and modelled using a second-order polynomial, both linear and quadratic terms were retained, indicating a non-linear response consistent with threshold-like limits on propagule supply. Thus, dispersal limitation contributes to diversity decline, although its form depends on the degree to which remoteness is parameterized. This pattern aligns with modified equilibrium-theory frameworks that explicitly incorporate dispersal filtering and propagule pressure (MacArthur and Wilson 1967; Weigelt and Kreft 2013).

Island area, by contrast, was not a significant predictor in either modelling framework. This apparent weakening of the species–area relationship likely reflects the Kurils' spatial configuration: the largest islands occur near the chain's ends, close to mainland source regions (Hokkaido and Kamchatka), and thus experience substantially higher immigration rates than similarly sized but centrally located islands. Consequently, isolation and volcanic activity override area per se, a contingency also reported in other archipelagos where geographic context modulates classical area effects (Lomolino 2000).

4.1.3 | H3 Elevation as a Compensatory Mechanism

Maximal elevation acts as a nuanced, yet consistently positive, modifier of SR across the Kurils. Both linear and polynomial models revealed an increase in SR with rising *elevation*, supporting the long-standing view that vertical gradients multiply habitat types and microclimates (Körner 2007; Stein et al. 2014). In effect, high elevation and topographical complexity compress a latitudinal spectrum into a single island: south-facing slopes may host thermophilic forest elements, whereas cloud-immersed ridges exposed to the cold Pacific Ocean a few kilometres away support alpine flora assemblages (Steinbauer et al. 2016).

Southern high-relief islands such as Iturup (Figure S3) exemplify this 'vertical zoning' by sustaining montane tundra taxa otherwise confined to the northern Kurils (Barkalov 2009). Such elevational refugia may buffer climate-driven turnover, allowing cold-adapted lineages to persist locally even as regional temperatures rise. In that sense, maximal elevation acts as a compensatory mechanism that boosts SR beyond what the main climatic gradient and island size alone would predict.

Notably, *elevation* did not significantly influence either SES.MNTD or SES.MPD. This decoupling indicates that the positive effect of *elevation* on SR is not accompanied by detectable

changes in phylogenetic relatedness among co-occurring species. In other words, topographic complexity appears to increase taxonomic diversity without systematically promoting either phylogenetic clustering or overdispersion (Stevens et al. 2012). This pattern underscores that taxonomic and phylogenetic diversity, though often correlated, can respond differently to the same environmental gradient.

Vegetation heterogeneity itself was not retained as a primary predictor, likely because it largely reflects the underlying climatic and geological template rather than acting as an independent driver. This is consistent with the view that habitat diversity often emerges as a response to macro-environmental constraints, rather than functioning as an autonomous determinant of SR (Stein et al. 2014).

4.2 | Inter-Dependencies and Model Performance

The modelling results support the complexity of predictor interactions. The stepwise linear model explains 93% of the variance in SR (adjusted $R^2 = 0.934$), but model comparison favoured a polynomial model that allowed for non-linear effects and reduced multicollinearity. The polynomial model showed stronger support and slightly improved explanatory power (adjusted $R^2 = 0.938$), highlighting the importance of flexible modelling frameworks when environmental gradients covary. Threshold-like effects of predictors, captured by polynomial terms, suggest that strict linear approaches may obscure meaningful saturation points.

SEMs further clarified causal pathways: *latitude* and *volcanity* exert predominantly direct negative effects on SR, whereas *elevation* enhances SR partly by increasing habitat heterogeneity. The island area has only a minor independent effect once volcanic activity (Whittaker et al. 2017) and habitat heterogeneity (Stein et al. 2014) are considered. Overall, the SEMs corroborated the multiple-regression results: latitudinal gradient, volcanic activity and geographic isolation were the dominant constraints on the Kurils Islands' floras, whereas island size did not exert a significant direct effect on SR or phylogenetic structure once other predictors were included.

Taken together, our results emphasise the limits of island size–remoteness models used on their own. Island size and distance to the mainland remain useful basic predictors, but their influence is modulated by climatic gradient, island volcanic activity and topographic complexity. The Kurils confirm the primacy of macroecological gradients, such as latitude-driven climate, in structuring both taxonomic and phylogenetic diversity (Hawkins et al. 2003; Kreft et al. 2008; Willig et al. 2003).

From a conservation standpoint, the mid-chain Kuril Islands are doubly vulnerable: their small size, remoteness and high volcanic activity constrain both colonisation and persistence of vascular plants. Southern and northern 'source' islands, although they host more species, face mounting anthropogenic pressures and climate warming effects, for example, shifting of vegetation belts and potential extinction of cold-tolerant alpine taxa (Gonzalez et al. 2010).

4.3 | Final Remarks

We evaluated three island-biogeography expectations in a temperate–subarctic, volcanically active system. First (H1), we documented strong latitudinal filtering: SR, SES.MNTD and SES.MPD all declined poleward, and the floristic transition from East Asian to Asian–American and circumpolar elements was driven primarily by species turnover rather than nested species loss. Second (H2), small, remote and highly volcanic islands in the central Kurils formed a pronounced taxonomic and phylogenetic bottleneck. SEMs identified direct negative effects of volcanic activity and geographic isolation, while polynomial regressions revealed a non-linear isolation threshold beyond which additional remoteness produced little further loss in SR, highlighting limits to propagule supply. Third (H3), maximal elevation consistently increased SR, likely by increasing vertical environmental heterogeneity, but it did not measurably affect phylogenetic structure. This decoupling indicates that topographic complexity can partially mitigate climatic and volcanic constraints on SR without substantially expanding evolutionary breadth.

5 | Conclusion

Our findings tie together the island-biogeographic concepts: while MacArthur and Wilson's equilibrium framework helps explain baseline area–distance effects, the Kuril Islands arc demonstrates that latitude-driven climate severity, volcanic activity and non-linear isolation set both SR and phylogenetic diversity. At the same time, habitat heterogeneity (in the form of elevational zonation and successional mosaics, sometimes supported by the active volcanism) partially offsets these harsh filters by expanding niche space, in line with the emerging NTIB. Thus, volcanic archipelagos like the Kurils serve not only as tests of the ETIB but also as historical and niche-centric perspectives on how islands generate and sustain biodiversity.

Author Contributions

Kirill Korznikov: conceptualisation, data curation, investigation, formal analysis, methodology, visualisation, writing – original draft preparation (equal), writing – review and editing. **Vyacheslav Barkalov:** conceptualisation, data curation, investigation (lead), methodology, validation, writing – review and editing. **Pavel Fibich:** formal analysis, software, validation, writing – review and editing. **Jan Altman:** funding acquisition, validation, writing – review and editing. **Jiří Doležal:** conceptualisation, funding acquisition, methodology, validation, visualisation, writing – original draft preparation (equal), writing – review and editing.

Acknowledgements

This work was supported by grants from the Czech Science Foundation (GA24-11954S and 25-15727S), the scientific framework of the Federal Scientific Center for the Biodiversity of Terrestrial Biota of East Asia FEB RAS (N 124012400285-7) and the long-term research development project RVO 67985939 of the Czech Academy of Sciences. Field permits were not required for the fieldworks conducted in this study. Open access publishing facilitated by Botanicky ustav Akademie ved Ceske republiky, as part of the Wiley - CzechELib agreement.

Funding

This work was supported by Grantová Agentura České Republiky (24-11954S, 25-15727S); Federal Scientific Center for the Biodiversity of Terrestrial Biota of East Asia FEB RAS (124012400285-7); and Institute of Botany of the Czech Academy of Sciences (RVO 67985939).

Conflicts of Interest

The authors declare no conflicts of interest.

Data Availability Statement

Quantitative data on Kuril Islands species richness, phylogenetic diversity, and all predictor variables are provided in the Supporting Information. A ready-to-analyse island-level dataset (species richness, SES.MNTD, SES.MPD and all predictor variables), together with the island × species matrix, is available on Zenodo: https://doi.org/10.5281/zenodo.18835010. The underlying raw floristic checklist used to compile the datasets is available from the authors upon reasonable request. An earlier version of this checklist (without recent updates and additional records) was published in Flora of the Kuril Islands (Barkalov 2009). The R scripts used for all analyses are also available on Zenodo: https://doi.org/10.5281/zenodo.18835010.

References

Allen, A. P., J. H. Brown, and J. F. Gillooly. 2002. "Global Biodiversity, Biochemical Kinetics, and the Energetic-Equivalence Rule." *Science* 297, no. 5586: 1545–1548. https://doi.org/10.1126/science.1072380.

Atlas of the Kuril Islands. 2009. *Atlas of the Kuril Islands*. Institute of Geography RAS.

Barkalov, V. Y. 2009. *Flora of the Kuril Islands*. Dalnauka.

Barkalov, V. Y., and V. V. Yakubov. 2007. "*Psilotum nudum* (Psilotaceae), a New Species to the Flora of Russia From the Kuril Islands." *Botanicheskii Zhurnal* 92, no. 12: 1946–1948.

Baselga, A. 2010. "Partitioning the Turnover and Nestedness Components of Beta Diversity." *Global Ecology and Biogeography* 19, no. 1: 134–143. https://doi.org/10.1111/j.1466-8238.2009.00490.x.

Beaugrand, G., L. Kléparski, C. Luczak, E. Goberville, and R. R. Kirby. 2024. "A Niche-Based Theory of Island Biogeography." *Ecology and Evolution* 14, no. 6: e11540. https://doi.org/10.1002/ece3.11540.

Beck, H. E., N. E. Zimmermann, T. R. McVicar, N. Vergopolan, A. Berg, and E. F. Wood. 2018. "Present and Future Köppen–Geiger Climate Classification Maps at 1-km Resolution." *Scientific Data* 5: 180214. https://doi.org/10.1038/sdata.2018.214.

Bhatta, K. P., O. Mottl, V. A. Felde, et al. 2024. "Latitudinal Gradients in the Phylogenetic Assembly of Angiosperms in Asia During the Holocene." *Scientific Reports* 14, no. 1: 17940. https://doi.org/10.1038/s41598-024-67650-1.

Blackburn, T. M., S. Delean, P. Pyšek, and P. Cassey. 2016. "On the Island Biogeography of Aliens: A Global Analysis of the Richness of Plant and Bird Species on Oceanic Islands." *Global Ecology and Biogeography* 25, no. 7: 859–868. https://doi.org/10.1111/geb.12339.

Borregaard, M. K., T. J. Matthews, and R. J. Whittaker. 2016. "The General Dynamic Model: Towards a Unified Theory of Island Biogeography?" *Global Ecology and Biogeography* 25, no. 7: 805–816. https://doi.org/10.1111/geb.12348.

Carlquist, S. 1974. *Island Biology*. Columbia University Press.

Cavender-Bares, J., K. H. Kozak, P. V. A. Fine, and S. W. Kembel. 2009. "The Merging of Community Ecology and Phylogenetic Biology." *Ecology Letters* 12, no. 7: 693–715. https://doi.org/10.1111/j.1461-0248.2009.01314.x.

De Grave, J., F. I. Zhimulev, S. Glorie, et al. 2015. "Late Palaeogene Emplacement and Late Neogene–Quaternary Exhumation of the Kuril Island-Arc Root (Kunashir Island) Constrained by Multi-Method Thermochronometry." *Geoscience Frontiers* 33: 1–10. https://doi.org/10.1016/j.gsf.2015.05.002.

Emerson, B. C., and N. Kolm. 2005. "Species Diversity Can Drive Speciation." *Nature* 434, no. 7036: 1015–1017. https://doi.org/10.1038/nature03450.

Erlandson, J. M., and T. J. Braje. 2011. "From Asia to the Americas by Boat? Paleogeography, Paleoecology, and Stemmed Points of the Northwest Pacific." *Quaternary International* 239, no. 1: 28–37. https://doi.org/10.1016/j.quaint.2011.02.030.

Fick, S. E., and R. J. Hijmans. 2017. "WorldClim 2: New 1-km Spatial Resolution Climate Surfaces for Global Land Areas." *International Journal of Climatology* 37, no. 12: 4302–4315. https://doi.org/10.1002/joc.5086.

Fox, J., and S. Weisberg. 2019. *An R Companion to Applied Regression*. Third ed. Sage. https://www.john-fox.ca/Companion/.

Friedman, J., T. Hastie, and R. Tibshirani. 2010. "Regularization Paths for Generalized Linear Models via Coordinate Descent." *Journal of Statistical Software* 33, no. 1: 1–22. https://doi.org/10.18637/jss.v033.i01.

Friedman, J., T. Hastie, and R. Tibshirani. 2025. "glmnet: Lasso and Elastic-Net Regularized Generalized Linear Models. R Package Version 4.1–10." https://cran.r-project.org/web/packages/glmnet/.

Garroutte, M., F. Huettmann, C. O. Webb, and S. M. Ickert-Bond. 2018. "Biogeographic and Anthropogenic Correlates of Aleutian Islands Plant Diversity: A Machine-Learning Approach." *Journal of Systematics and Evolution* 56, no. 5: 476–497. https://doi.org/10.1111/jse.12456.

Gillespie, R. G., E. M. Claridge, and G. K. Roderick. 2008. "Biodiversity Dynamics in Isolated Island Communities: Interaction Between Natural and Human-Mediated Processes." *Molecular Ecology* 17, no. 1: 45–57. https://doi.org/10.1111/j.1365-294X.2007.03466.x.

Gjesfjeld, E., M. A. Etnier, K. Takase, W. A. Brown, and B. Fitzhugh. 2019. "Biogeography and Adaptation in the Kuril Islands, Northeast Asia." *World Archaeology* 51, no. 3: 429–453. https://doi.org/10.1080/00438243.2019.1715248.

Gonzalez, P., R. P. Neilson, J. M. Lenihan, and R. J. Drapek. 2010. "Global Patterns in the Vulnerability of Ecosystems to Vegetation Shifts due to Climate Change." *Global Ecology and Biogeography* 19, no. 6: 755–768. https://doi.org/10.1111/j.1466-8238.2010.00558.x.

Grace, J. B., T. M. Anderson, H. Olff, and S. M. Scheiner. 2010. "On the Specification of Structural Equation Models for Ecological Systems." *Ecological Monographs* 80: 67–87. https://doi.org/10.1890/09-0464.1.

Graham, S. E., J. P. Loveless, and B. J. Meade. 2018. "Global Plate Motions and Earthquake Cycle Effects." *Geochemistry, Geophysics, Geosystems* 19, no. 7: 2032–2048. https://doi.org/10.1029/2017GC007391.

Hawkins, B. A., R. Field, H. V. Cornell, et al. 2003. "Energy, Water, and Broad-Scale Geographic Patterns of Species Richness." *Ecology* 84, no. 12: 3105–3117. https://doi.org/10.1890/03-8006.

Helmus, M. R., D. L. Mahler, and J. B. Losos. 2014. "Island biogeography of the Anthropocene." *Nature* 513, no. 7519: 543–546. https://doi.org/10.1038/nature13739.

Jin, Y., and H. Qian. 2019. "V.PhyloMaker: An R Package That Can Generate Very Large Phylogenies for Vascular Plants." *Ecography* 42, no. 8: 1353–1359. https://doi.org/10.1111/ecog.04434.

Jonsson, M., G. Englund, and D. A. Wardle. 2011. "Direct and Indirect Effects of Area, Energy and Habitat Heterogeneity on Breeding Bird Communities." *Journal of Biogeography* 38: 1186–1196. https://doi.org/10.1111/j.1365-2699.2010.02470.x.

Kembel, S. W., P. D. Cowan, M. R. Helmus, et al. 2010. "Picante: R Tools for Integrating Phylogenies and Ecology." *Bioinformatics* 26, no. 11: 1463–1464. https://doi.org/10.1093/bioinformatics/btq166.

Kisel, Y., and T. G. Barraclough. 2010. "Speciation Has a Spatial Scale That Depends on Levels of Gene Flow." *American Naturalist* 175, no. 3: 316–334. https://doi.org/10.1086/650369.

Körner, C. 2007. "The Use of 'Altitude' in Ecological Research." *Trends in Ecology & Evolution* 22, no. 11: 569–574. https://doi.org/10.1016/j.tree.2007.09.006.

Kreft, H., W. Jetz, J. Mutke, G. Kier, and W. Barthlott. 2008. "Global Diversity of Island Floras From a Macroecological Perspective." *Ecology Letters* 11, no. 2: 116–127. https://doi.org/10.1111/j.1461-0248.2007.01129.x.

Lefcheck, J. S. 2016. "piecewiseSEM: Piecewise Structural Equation Modelling in r for Ecology, Evolution, and Systematics." *Methods in Ecology and Evolution* 7, no. 5: 573–579. https://doi.org/10.1111/2041-210X.12512.

Lim, J. Y., and C. R. Marshall. 2017. "The True Tempo of Evolutionary Radiation and Decline Revealed on the Hawaiian Archipelago." *Nature* 543, no. 7647: 710–713. https://doi.org/10.1038/nature21675.

Lomolino, M. V. 2000. "Ecology's Most General, Yet Protean Pattern: The Species-Area Relationship." *Journal of Biogeography* 27, no. 1: 17–26. https://doi.org/10.1046/j.1365-2699.2000.00377.x.

MacArthur, R. H., and E. O. Wilson. 1967. *The Theory of Island Biogeography*. Princeton University Press.

MacDonald, Z. G., I. D. Anderson, J. H. Acorn, and S. E. Nielsen. 2018. "The Theory of Island Biogeography, the Sample-Area Effect, and the Habitat Diversity Hypothesis: Complementarity in a Naturally Fragmented Landscape of Lake Islands." *Journal of Biogeography* 45, no. 12: 2730–2743. https://doi.org/10.1111/jbi.13460.

Morrison, L. W. 2010. "Long-Term Non-Equilibrium Dynamics of Insular Floras: A 17-Year Record." *Global Ecology and Biogeography* 19, no. 5: 663–672. https://doi.org/10.1111/j.1466-8238.2010.00543.x.

Nakamura, Y., P. V. Krestov, and A. M. Omelko. 2007. "Bioclimate and Zonal Vegetation in Northeast Asia: First Approximation to an Integrated Study." *Phytocoenologia* 37: 443–470. https://doi.org/10.1127/0340-269X/2007/0037-0443.

Nogales, M., M. Guerrero-Campos, T. Boulesteix, et al. 2022. "The Fate of Terrestrial Biodiversity During an Oceanic Island Volcanic Eruption." *Scientific Reports* 12, no. 1: 19344. https://doi.org/10.1038/s41598-022-22863-0.

Oksanen, J., G. L. Simpson, F. G. Blanchet, et al. 2022. "vegan: Community Ecology Package (Version 2.6-4)." https://CRAN.R-project.org/package=vegan.

Pianka, E. R. 1966. "Latitudinal Gradients in Species Diversity: A Review of Concepts." *American Naturalist* 100, no. 910: 33–46. https://doi.org/10.1086/282398.

Pietsch, T. W., V. V. Bogatov, K. Amaoka, et al. 2003. "Biodiversity and Biogeography of the Islands of the Kuril Archipelago." *Journal of Biogeography* 30, no. 9: 1297–1310. https://doi.org/10.1046/j.1365-2699.2003.00956.x.

POWO. 2025. *Plants of the World Online*. Royal Botanic Gardens, Kew. https://powo.science.kew.org/.

Price, J. P., and D. A. Clague. 2002. "How Old Is the Hawaiian Biota? Geology and Phylogeny Suggest Recent Divergence." *Proceedings of the Royal Society of London, Series B: Biological Sciences* 269, no. 1508: 2429–2435. https://doi.org/10.1098/rspb.2002.2175.

Qian, H., S. Qian, J. Zhang, and M. Kessler. 2024. "Effects of Climate and Environmental Heterogeneity on the Phylogenetic Structure of Regional Angiosperm Floras Worldwide." *Nature Communications* 15, no. 1: 1079. https://doi.org/10.1038/s41467-024-45155-9.

Qian, H., and R. E. Ricklefs. 2007. "A Latitudinal Gradient in Large-Scale Beta Diversity for Vascular Plants in North America." *Ecology Letters* 10, no. 8: 737–744. https://doi.org/10.1111/j.1461-0248.2007.01066.x.

R Core Team. 2025. *R: A Language and Environment for Statistical Computing*. R Foundation for Statistical Computing. https://www.r-project.org/.

Razjigaeva, N. G., L. A. Ganzey, T. A. Grebennikova, et al. 2013. "Holocene Climatic Changes and Vegetation Development in the Kuril Islands." *Quaternary International* 290: 126–138. https://doi.org/10.1016/j.quaint.2012.06.034.

Romanyuk, F., and A. Degterev. 2020. "Transformation of the Coastline of Raikoke Island After the Explosive Eruption on June 21–25, 2019 (Central Kuril Islands)." *Geosystems of Transition Zones* 4: 351–358. https://doi.org/10.30730/gtrz.2020.4.3.351-358.

Romanyuk, F., and A. Kordyukov. 2021. "Vegetation Cover of the Lahar Valley on the Sarychev Peak Volcano (Matua Isl., Middle Kuril Islands) After the Eruption in 2009: Current State and Features of Succession Processes." *Journal of Mountain Science* 18: 1762–1777. https://doi.org/10.1007/s11629-020-6437-0.

Stein, A., K. Gerstner, and H. Kreft. 2014. "Environmental Heterogeneity as a Universal Driver of Species Richness Across Taxa, Biomes and Spatial Scales." *Ecology Letters* 17, no. 7: 866–880. https://doi.org/10.1111/ele.12277.

Steinbauer, M. J., R. Field, J.-A. Grytnes, et al. 2016. "Topography-Driven Isolation, Speciation and a Global Increase of Endemism With Elevation." *Global Ecology and Biogeography* 25, no. 9: 1097–1107. https://doi.org/10.1111/geb.12469.

Stevens, R. D., M. M. Gavilanez, J. S. Tello, and D. A. Ray. 2012. "Phylogenetic Structure Illuminates the Mechanistic Role of Environmental Heterogeneity in Community Organization." *Journal of Animal Ecology* 81, no. 2: 455–462. https://doi.org/10.1111/j.1365-2656.2011.01900.x.

Stracey, C. M., and S. L. Pimm. 2009. "Testing Island Biogeography Theory With Visitation Rates of Birds to British Islands." *Journal of Biogeography* 36, no. 8: 1532–1539. https://doi.org/10.1111/j.1365-2699.2009.02090.x.

Tatewaki, M. 1957. "Geobotanical Study on the Kurile Islands." *Acta Horti Gothoburgensis* 21, no. 2: 43–123.

Thórhallsdóttir, T. E. 2021. "The Vascular Floras of High-Latitude Islands With Special Reference to Iceland." In *Biogeography in the Sub-Arctic: The Past and Future of North Atlantic Biota*, edited by E. Panagiotakopulu and J. P. Sadler, 113–146. John Wiley & Sons. https://doi.org/10.1002/9781118561461.ch6.

Vascular Plants of the Soviet (Russian) Far East. 1985–1996. *Vascular Plants of the Soviet (Russian) Far East*. Vol. 1–8. Dalnauka.

Venables, W. N., and B. D. Ripley. 2002. *Modern Applied Statistics With S*. 4th ed. Springer.

Weigelt, P., and H. Kreft. 2013. "Quantifying Island Isolation – Insights From Global Patterns of Insular Plant Species Richness." *Ecography* 36, no. 4: 417–429. https://doi.org/10.1111/j.1600-0587.2012.07669.x.

Whittaker, R. J., J. M. Fernández-Palacios, T. J. Matthews, M. K. Borregaard, and K. A. Triantis. 2017. "Island Biogeography: Taking the Long View of Nature's Laboratories." *Science* 357, no. 6354: eaam8326. https://doi.org/10.1126/science.aam8326.

Whittaker, R. J., K. A. Triantis, and R. J. Ladle. 2008. "A General Dynamic Theory of Oceanic Island Biogeography." *Journal of Biogeography* 35, no. 6: 977–994. https://doi.org/10.1111/j.1365-2699.2008.01892.x.

Wickham, H. 2016. *ggplot2. In Use R!* Springer International Publishing. https://doi.org/10.1007/978-3-319-24277-4.

Willig, M. R., D. M. Kaufman, and R. D. Stevens. 2003. "Latitudinal Gradients of Biodiversity: Pattern, Process, Scale, and Synthesis." *Annual Review of Ecology, Evolution, and Systematics* 34: 273–309. https://doi.org/10.1146/annurev.ecolsys.34.012103.144032.

Supporting Information

Additional supporting information can be found online in the Supporting Information section. **Data S1:** jbi70194-sup-0001-supinfo01.pdf. **Figure S1:** Floristic survey coverage (red dashed lines) and long-term field camp locations (circles) across Kunashir Island. **Figure S2:** Floristic survey coverage (red dashed lines) and long-term field camp locations (circles) across Shikotan Island. **Figure S3:** Floristic survey coverage (red dashed lines) and long-term field camp locations (circles) across Iturup Island. **Figure S4:** Floristic survey coverage (red dashed lines) and long-term field camp locations (circles) across Urup, Brat Chirpoev and Chirpoy islands. **Figure S5:** Floristic survey coverage (red dashed lines) and long-term field camp locations (circles) across Simushir and Ketoy islands. **Figure S6:** Floristic survey coverage (red dashed lines) and long-term field camp locations (circles) across Ushishir, Rashua, Matua and Raykoke islands. **Figure S7:** Floristic survey coverage (red dashed lines) and long-term field camp locations (circles) across Shiashkotan, Kharimkotan and Onekotan islands. **Figure S8:** Floristic survey coverage (red dashed lines) and long-term field camp locations (circles) across Paramushir, Shumshu and Atlasova islands. **Figure S9:** Relationships between latitude and key climatic and geographic predictors across the Kuril Islands. **Figure S10:** Pearson correlation coefficients among predictors. **Figure S11:** Fitted responses of the Kuril Islands vascular species richness to maximal elevation (*elevation*). **Figure S12:** Fitted responses of phylogenetic diversity of vascular plant assemblages on the Kuril Islands, expressed as standardised mean nearest taxon distance (SES.MNTD) and standardised mean pairwise distance (SES.MPD), to the environmental gradients of island size (*area*), maximal elevation (*elevation*) and *isolation*. **Figure S13:** Diagnostic comparison of species richness regression models. **Figure S14:** Diagnostic comparison of SES.MNTD regression models. **Figure S15:** Diagnostic comparison of SES.MPD regression models. **Figure S16:** Structural-equation models (SEMs) linking all predictor variables to species richness and phylogenetic diversity metrics on the 20 main Kuril Islands; arrows represent relationships, red—positive effect, blue—negative effect; numbers near arrows are significant standardised path coefficients (β). **Table S1:** Comparison of linear and second-order polynomial bivariate models (AICc and nested *F*-tests) for environmental predictors of species richness and phylogenetic diversity. **Table S2:** Phytogeographical distribution types of vascular plant species. **Table S3:** The first structural equation model results for species richness (SR), standardised mean nearest taxon distance (SES.MNTD) and standardised mean pairwise distance (SES.MPD). **Table S4:** The second structural equation model results for species richness (SR), standardised mean nearest taxon distance (SES.MNTD) and standardised mean pairwise distance (SES.MPD).